A Mandelpinski Maze for Rational Maps of the Form $z^n + \lambda/z^d$ *†

Robert L. Devaney‡
Department of Mathematics
Boston University
111 Cummington Mall
Boston, MA 02215 USA

May 26, 2015

*Dedicated to Henk Broer on the occasion of his 65th Birthday.

†2000 MSC number: Primary 37F10; Secondary 37F45

‡Robert L. Devaney was partially supported by Simons Foundation Grant #208780

Abstract

In this paper we identify a new type of structure that lies in the parameter plane of the family of maps $z^n + \lambda/z^d$ where $n \geq 2$ is even but $d \geq 3$ is odd. We call this structure a Mandelbrot-Sierpinski maze. Basically, the maze consists at the first level of an infinite string of alternating Mandelbrot sets and Sierpinski holes that lie along an arc in the parameter plane for this family. At the next level, there are infinitely many smaller Mandelbrot sets and Sierpinski holes that alternate on the arc between each Mandelbrot set and Sierpinski hole on the previous level, and then finitely many other Mandelbrot sets and Sierpinski holes that extend away from the given Mandelbrot set in a pair of different directions. And then this structure repeats inductively to produce the "Mandelpinski" maze.

In this paper we will concentrate on the family of maps $F_\lambda(z) = z^n + \lambda/z^d$ where $n, d \geq 2$. It is known that there are several different and very interesting geometric structures surrounding the negative real axis in the parameter planes for these maps. For example, when n and d are even, it has been shown in [4] that there is a "Cantor necklace" that lies along the negative real axis in the parameter plane and a "principal" Mandelbrot set along the positive axis. A Cantor necklace is a set that is a continuous image of the Cantor middle-thirds set to which is adjoined countably many open disks in the plane in place of the removed open intervals along the real line. For parameters inside these open disks (which we call Sierpinski holes), the Julia set of F_λ is known to be a Sierpinski curve (i.e., is homeomorphic to the Sierpinski carpet fractal), and the different dynamical behaviors on these Julia sets is completely understood [12]. When n is odd and d is even, there is no such Cantor necklace; rather there are now two "principal" Mandelbrot sets, one along the positive real axis and the other along the negative real axis. As a consequence, the dynamical behavior for these parameters is very different from the behavior when n and d is even. Thus the remaining case is when n is even and d is odd; this too is a very different case that we shall

deal with in this paper.

As when d is even, we again have a principal Mandelbrot set straddling the positive real axis. But the structure on and around the negative real axis is very different. We shall show that there is a "Mandelpinski maze" (an MS-maze) in a neighborhood of the negative real axis in the parameter plane. Roughly speaking, this is a set that consists of infinitely many baby Mandelbrot sets and Sierpinski holes that alternate along a specific planar graph that has infinitely many vertices.

1 Preliminaries

In this paper we consider the family of rational maps given by

$$F_\lambda(z) = z^n + \frac{\lambda}{z^d}$$

where $n \geq 2$ is even and $d \geq 3$ is odd. When $|z|$ is large, we have that $|F_\lambda(z)| > |z|$, so the point at ∞ is an attracting fixed point in the Riemann sphere. We denote the immediate basin of attraction of ∞ by B_λ. There is also a pole at the origin for each of these maps, and so there is a neighborhood of the origin that is mapped into B_λ. If the preimage of B_λ surrounding the origin is disjoint from B_λ, we call this region the trap door and denote it by T_λ.

The Julia set of F_λ, $J(F_\lambda)$, has several equivalent definitions. $J(F_\lambda)$ is the set of all points at which the family of iterates of F_λ fails to be a normal family in the sense of Montel. Equivalently, $J(F_\lambda)$ is the closure of the set of repelling periodic points of F_λ, and it is also the boundary of the set of all points whose orbits tend to ∞ under iteration of F_λ, not just those in the boundary of B_λ. See [11].

One checks easily that there are $n+d$ critical points that are given by

$$c^\lambda = \left(\frac{d\lambda}{n}\right)^{\frac{1}{n+d}}$$

with the corresponding critical values given by

$$v^\lambda = \frac{(d+n)\lambda^{\frac{n}{n+d}}}{d^{\frac{d}{n+d}} n^{\frac{n}{n+d}}}.$$

There are also $n+d$ prepoles given by

$$p^\lambda = (-\lambda)^{\frac{1}{n+d}}.$$

The straight ray extending from the origin to ∞ and passing through the critical point c^λ is called the *critical point ray*. This ray is mapped two-to-one onto the portion of the straight ray from the origin to ∞ that starts at the critical value $F_\lambda(c^\lambda)$ and extends to ∞ beyond this critical value. A similar straight line extending from 0 to ∞ and passing through a prepole p^λ is a *prepole ray*, and this ray is mapped one-to-one onto the entire straight line passing through both the origin and the point $(-\lambda)^{n/(n+d)}$.

Let ω be an $(n+d)^{\text{th}}$ root of unity. Then we have $F_\lambda(\omega z) = \omega^n F_\lambda(z)$, and so it follows that the dynamical plane is symmetric under the rotation $z \mapsto \omega z$. In particular, all of the critical orbits have "similar" fates. If one critical orbit tends to ∞, then all must do so. If one critical orbit tends to an attracting cycle of some period, then all other critical orbits also tend to an attracting cycle, though these other cycles may have different periods. Nonetheless, the points on these attracting cycles are all symmetrically located with respect to the rotation by ω. As a consequence, each of B_λ, T_λ, and $J(F_\lambda)$ are symmetric under rotation by ω. Similarly, one checks easily that the parameter plane is symmetric under the rotation $\lambda \mapsto \nu\lambda$ where ν is an $(n-1)^{\text{st}}$ root of unity. The parameter plane is also symmetric under complex conjugation $\lambda \mapsto \overline{\lambda}$.

There is an Escape Trichotomy [6] for this family of maps. The first scenario in this trichotomy occurs when one and hence, by symmetry, all of the critical values lie in B_λ. In this case it is known that $J(F_\lambda)$ is a Cantor set. The corresponding set of λ-values in the parameter plane is denoted by $\mathcal{C}$ and called the Cantor set locus. The second scenario is that the critical values all lie in T_λ (which we assume is disjoint from B_λ). In this case the Julia set is a Cantor set of simple closed curves surrounding the origin. This can only happen when $n, d \geq 2$ but not both equal to 2 [10]. We call the region $\mathcal{E}^1$ in parameter plane where this occurs the "McMullen domain"; it is known that $\mathcal{E}^1$ is an open disk surrounding the origin [2]. The third scenario is that the orbit of a critical point enters T_λ at iteration 2 or higher. Then, by the above symmetry, all such critical orbits do the same. In this case, it is known that the Julia set is a Sierpinski curve [5], i.e., a set that is homeomorphic to the well known Sierpinski carpet fractal. The regions in the parameter plane for which this happens are the open disks that we call Sierpinski holes [13]. If the critical orbits do not escape to ∞, then it is known [7] that the Julia set is a connected set. Thus we call the set of parameters for which the critical orbits either do not escape or else enter the trap door at iteration 2 or higher the connectedness locus. This is the region between $\mathcal{C}$ and $\mathcal{E}^1$. See Figure 1.

In [1] it has been shown that there are $n-1$ principal Mandelbrot sets in the parameter plane for these maps. These are symmetrically located by the rotation νz around the origin and extend from the Cantor set locus down to the McMullen domain.

For more details about the dynamical properties of these maps and the structure of the parameter plane, see [3].

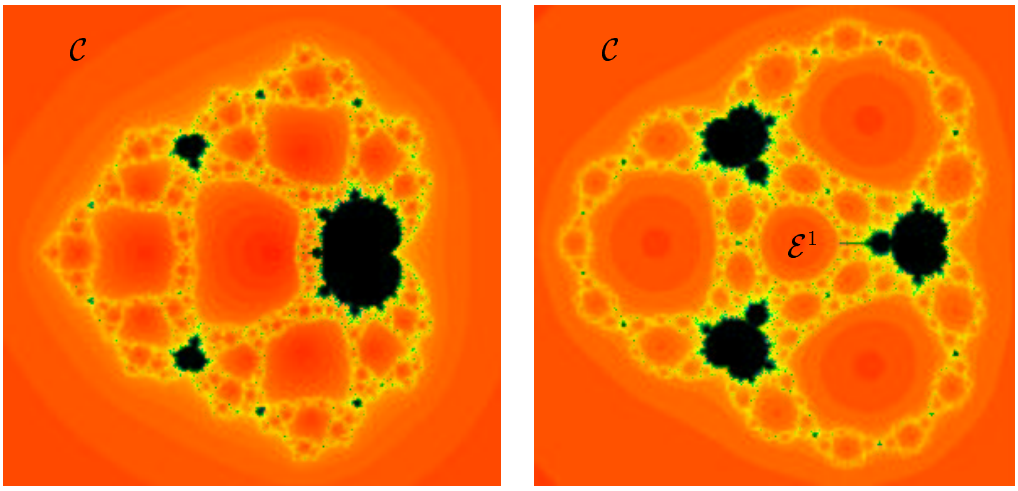

Figure 1: The parameter planes for the family $z^n + \lambda/z^d$ when $n = 2, d = 3$ and $n = 4, d = 3$. There is one principal Mandelbrot set in the first case and three symmetrically located such sets in the second. All of the red holes in these pictures (except the one surrounding the origin) are Sierpinski holes. $\mathcal{E}^1$ is too small to be seen in the first figure.

2 Phase One of the Construction of the MS-Maze

For most of the remainder of this paper, we shall concentrate for simplicity on the special family

$$F_\lambda(z) = z^2 + \frac{\lambda}{z^3}.$$

At the end of the paper we will sketch the minor modifications necessary to extend the results to the more general case where $n \geq 2$ is even and $d \geq 3$ is odd.

There are now five critical points for the map F_λ given by $(3\lambda/2)^{1/5}$. We denote the critical point that lies in $\mathbb{R}^-$ when $\lambda \in \mathbb{R}^-$ by $c_0 = c_0^\lambda$ (and then c_0^λ varies analytically with λ). As λ moves half way around the origin from $\mathbb{R}^-$, c_0 rotates exactly one-tenth of a turn in the corresponding direction.

We denote the other critical points by $c_j = c_j^\lambda$ for $-2 \leq j \leq 2$ where the c_j are now arranged in the clockwise order as j increases. Note that, when $\operatorname{Arg} \lambda = 0$, c_2 lies in $\mathbb{R}^+$ and when $\operatorname{Arg} \lambda = 2\pi$, c_{-2} now lies in $\mathbb{R}^+$. The critical values of F_λ are then given by $v^\lambda = \kappa \lambda^{2/5}$ where κ is the constant given by $5/(2^{2/5}3^{3/5})$. One computes easily that $\kappa \approx 1.96$. We denote by v_j^λ the critical value that is the image of c_j^λ.

There are also five prepoles for F_λ given by $(-\lambda)^{1/5}$. We denote the prepole that lies in $\mathbb{R}^+$ when $\lambda \in \mathbb{R}^-$ by $p_2 = p_2^\lambda$. The other prepoles are denoted by $p_j = p_j^\lambda$ where again $-2 \leq j \leq 2$ and the p_j are arranged in the clockwise order as j increases. Note that, when $\lambda \in \mathbb{R}^-$, the critical point c_0 lies between the two prepole rays passing through p_0 and p_{-1}.

We now construct the initial portion of the MS maze. This will be what we call a "Sierpindelbrot" arc, or, for short, an SM arc. An SM arc is an arc in the parameter plane that passes alternately along the spines of either finitely or infinitely many baby Mandelbrot sets and through the centers of the same number of Sierpinski holes. By the spine of the Mandelbrot set we mean the analogue of the portion of the real axis lying in the usual Mandelbrot set associated with the quadratic family $z^2 + c$.

In this first SM arc, there will be infinitely many Mandelbrot sets $\mathcal{M}^k$ with $k \geq 2$ where k is the period of the attracting cycle for parameters drawn from the main cardioid of $\mathcal{M}^k$, i.e., the base period of $\mathcal{M}^k$. There will also be infinitely many Sierpinski holes $\mathcal{E}^k$ with $k \geq 1$ where k is the escape time in $\mathcal{E}^k$, i.e., the number of iterations it takes for the orbit of the critical points to enter T_λ. In this first case, the SM arc will be the portion of the negative real axis in the parameter plane extending from the McMullen domain down to the endpoint on the boundary of the connectedness locus. Then the Mandelbrot sets and Sierpinski holes will be arranged along this

arc as follows:

$$\ldots \mathcal{M}^4 < \mathcal{E}^3 < \mathcal{M}^3 < \mathcal{E}^2 < \mathcal{M}^2 < \mathcal{E}^1$$

where, as earlier, $\mathcal{E}^1$ denotes the McMullen domain. In each case there will be an interval of nonzero length between any adjacent Mandelbrot set and Sierpinski hole lying along this SM arc.

To construct the objects lying along this SM arc, we will restrict attention at first to the set of parameters in the annular region $\mathcal{O}$ given by $10^{-10} \leq |\lambda| \leq 2$. Also, let $\mathcal{A}$ be the annulus in the dynamical plane given by $\kappa 10^{-4} \leq |z| \leq \kappa 2^{2/5}$.

Proposition.

1. *For any $\lambda \in \mathcal{O}$, all points on the outer circular boundary of $\mathcal{A}$ lie in B_λ, while all points on the inner circular boundary of $\mathcal{A}$ lie in T_λ. Moreover, F_λ maps each of these boundaries strictly outside the boundary of $\mathcal{A}$.*

2. *If λ lies on the inner circular boundary of $\mathcal{O}$, then each critical value lies on the inner circular boundary of $\mathcal{A}$ and so λ lies in the McMullen domain.*

3. *If λ lies on the outer circular boundary of $\mathcal{O}$, then each critical value lies on the outer circular boundary of $\mathcal{A}$ and so λ lies in the Cantor set locus in the parameter plane.*

Proof: First, if $|z| = \tau\kappa 2^{2/5}$ for any $\tau \geq 1$, we have for each $\lambda \in \mathcal{O}$:

$$\begin{aligned} |F_\lambda(z)| &\geq |\tau^2\kappa^2 2^{4/5}| - \left|\frac{\lambda}{\tau^3\kappa^3 2^{6/5}}\right| \\ &\geq \tau^2 1.95^2 2^{4/5} - \frac{2}{\tau^3\kappa^3 2^{6/5}} \\ &\geq 6\tau^2 - 1/(7\tau^3) \\ &> \tau\kappa 2^{2/5} = |z|. \end{aligned}$$

So all points outside of the circle $|z| = \kappa 2^{2/5}$ lie in B_λ when $\lambda \in \mathcal{O}$.

Similarly, if $|z| = \kappa 10^{-4}$, then we have

$$|F_\lambda(z)| \geq \frac{|\lambda|}{\kappa^3 10^{-12}} - \kappa^2 10^{-8} \geq \frac{10^{-10}}{\kappa^3 10^{-12}} - \kappa^2 10^{-8} \geq 100/\kappa^2 - \epsilon$$

where $\epsilon \approx 4 \cdot 10^{-8}$. So this inner boundary is mapped into B_λ and outside of $\mathcal{A}$, and so are all smaller circles around the origin. Hence this circle lies in T_λ (when λ lies in the connectedness locus).

Now if λ lies on the inner circular boundary of $\mathcal{O}$, then $|\lambda| = 10^{-10}$ so that $|v^\lambda| = \kappa 10^{-4}$. Hence, for these λ-values, v^λ lies on the inner circular boundary of $\mathcal{A}$, which lies in T_λ, and λ therefore lies in the McMullen domain. If λ lies on the outer circular boundary of $\mathcal{O}$, then $|\lambda| = 2$ so that $|v^\lambda| = \kappa 2^{2/5}$ (the outer boundary of $\mathcal{A}$) and thus this boundary circle lies in the Cantor set locus in the parameter plane.

□

We now restrict attention to a "smaller" subset of $\mathcal{O}$. Let $\mathcal{O}'$ be the subset of $\mathcal{O}$ containing parameters λ for which $0 \leq \operatorname{Arg} \lambda \leq 2\pi$. Despite the overlap of this region along the real axis, we will think of $\mathcal{O}'$ as being a closed disk (not an annulus) in the parameter plane because, as $\operatorname{Arg} \lambda$ increases from 0 to 2π, the critical point c_0 that we will be following rotates one-fifth of a turn in the dynamical plane. So this point will migrate to the position of a different critical point as $\operatorname{Arg} \lambda$ rotates one full turn.

For any parameter in $\mathcal{O}'$, let L^λ be the closed "portion of the wedge" in the annulus $\mathcal{A}$ in the dynamical plane that is bounded by the two prepole rays through p_0 and p_{-1}. When $\lambda \in \mathbb{R}^-$, L^λ is thus bounded by the rays extending from 0 and passing through $\exp(2\pi i(2/5))$ and $\exp(2\pi i(3/5))$. So the critical point c_0 lies in the interior of L^λ. Next, let R^λ be the portion of the wedge in $\mathcal{A}$ that is bounded by the critical point rays passing through c_2 and c_{-2}. When $\lambda \in \mathbb{R}^-$, this wedge is bounded by the critical point rays

extending from 0 and passing through $\exp(\pm 2\pi i/10)$. Note that R^λ is the symmetric image of L^λ under $z \mapsto -z$. See Figure 2.

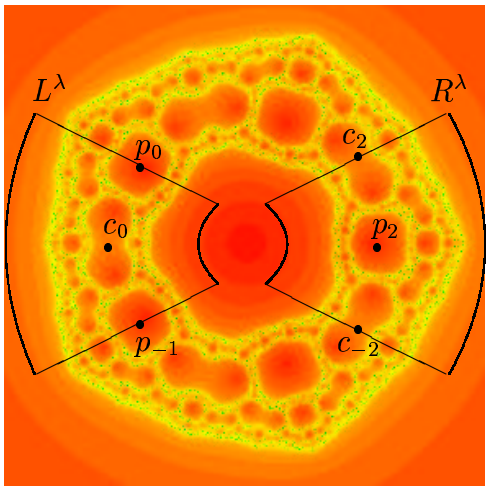

Figure 2: The wedges L^λ and R^λ for $\lambda = -0.09$.

Proposition. *For each $\lambda \in \mathcal{O}'$:*

1. *F_λ maps R^λ in one-to-one fashion onto a region that contains the interior of $R^\lambda \cup L^\lambda$ together with a portion of T_λ that contains 0;*

2. *F_λ maps L^λ two-to-one over a region that contains the interior of R^λ;*

3. *As λ winds once around the boundary of $\mathcal{O}'$, the critical value $F_\lambda(c_0^\lambda) = v_0^\lambda$ winds once around the boundary of R^λ, (i.e., the winding index of the vector connecting this critical value to the prepole p_2^λ lying in the interior of R^λ is one).*

Proof: For the first case, recall that the straightline boundaries of R^λ are mapped two-to-one onto the critical value rays passing through v_2^λ and v_{-2}^λ.

When $0 < \operatorname{Arg}\lambda < 2\pi$, one checks easily that these rays are disjoint from both R^λ and L^λ. The reason for this is that the arguments of the rays containing the critical values increase/decrease twice as fast as the arguments of the critical point and prepole rays as $\operatorname{Arg}\lambda$ varies. More precise details about this are given in Section 5. However, when $\operatorname{Arg}\lambda = 0$, the critical value ray v_2^λ now reaches the boundary of R^λ on the real line, and when $\operatorname{Arg}\lambda = 2\pi$, the same thing is true for the critical value ray v_{-2}^λ. By the previous Proposition, the outer boundary curve of R^λ is mapped to an arc that lies in B_λ and also lies outside the outer circular boundaries of R^λ and L^λ. This image arc connects the two critical value rays in B_λ, and lies to the right of these rays in the basin. The inner boundary is mapped to a similar arc connecting these rays but now lying to the left of L^λ. Consequently, the image of R^λ properly contains the interiors of both R^λ and L^λ. Since the criticl values never land on 0, the image of R^λ also properly contains a region in T_λ surrounding 0.

For the second case, we have that the straightline boundaries of L^λ contain the prepoles p_0^λ and p_{-1}^λ, which are both mapped to straight lines passing through the origin. In the case of p_0^λ, this straight line passes through $\exp(4\pi i/5)$ when $\lambda \in \mathbb{R}^-$. Then as $\operatorname{Arg}\lambda$ increases or decreases by at most π, the argument of this image line rotates by at most one-fifth of a turn in the corresponding direction. Hence this line lies strictly outside R^λ (except when $\operatorname{Arg}\lambda = 2\pi$, in which case this line is now the real axis) and so meets the boundary of R^λ. Similar arguments work for the image of the other prepole ray. For the circular boundaries of L^λ, by the previous Proposition, they are both mapped to curves in B_λ that lie outside of the outer boundary of $\mathcal{A}$, but now these curves are arcs that connect the images of the prepole rays passing to the right of these lines. Hence F_λ maps L^λ over R^λ in two-to-one fashion.

For the third case, when $\operatorname{Arg}\lambda = 0$, the image of c_0^λ lies on the ray

passing through $\exp(-2\pi i/5)$, and when $\operatorname{Arg}\lambda = 2\pi$, this critical value lies on the complex conjugate ray. So, for these parameters, the critical value lies on a line that includes the straight line boundary of R^λ. For the circular boundaries of $\mathcal{O}'$, the previous Proposition shows that the critical value now rotates around the corresponding circular boundary of R^λ. Hence the critical value $F_\lambda(c_0^\lambda)$ winds with index one around R^λ as λ winds around the boundary of $\mathcal{O}'$.

□

Before constructing the SM arc, we recall the concept of a polynomial-like map. Let G_μ be a family of holomorphic maps that depends analytically on the parameter μ lying in some open disk $\mathcal{D}$. Suppose each $G_\mu : U_\mu \to V_\mu$ where both U_μ and V_μ are open disks that also depend analytically on μ. G_μ is then said to be polynomial-like of degree 2 if, for each μ:

- G_μ maps U_μ two-to-one onto V_μ and so there is a unique critical point in U_μ;
- V_μ contains U_μ;
- As μ winds once around the boundary of $\mathcal{D}$, the critical value winds once around U_μ in the region $V_\mu - U_\mu$.

As shown in [9], for such a family of polynomial-like maps, there is a homeomorphic copy of the Mandelbrot set in the disk $\mathcal{D}$. Moreover, for μ-values in this Mandelbrot set, $G_\mu \,|\, U_\mu$ is conjugate to the corresponding quadratic map given by this homeomorphism.

We can now prove

Theorem. *There exists an SM arc along the negative real axis in the parameter plane that consists of infinitely many Mandelbrot sets $\mathcal{M}^k$ with $k \geq 2$ and infinitely many Sierpinski holes $\mathcal{E}^k$ with $k \geq 1$. Here k denotes the base*

period of $\mathcal{M}^k$ and the escape time of $\mathcal{E}^k$. These sets are arranged along the negative real axis in this manner:

$$\ldots \mathcal{E}^3 < \mathcal{M}^3 < \mathcal{E}^2 < \mathcal{M}^2 < \mathcal{E}^1.$$

Proof: We first consider the escape time case. By construction, for each $\lambda \in \mathcal{O}'$, there is a unique prepole p_2^λ in the interior of R^λ. Since F_λ maps R^λ one-to-one over itself, there is a unique preimage of this prepole, z_3^λ, in R^λ, so $F_\lambda^2(z_3^\lambda) = 0$. Continuing, for each $\lambda \in \mathcal{O}'$, there is a unique point z_k^λ in R^λ for which we have $F_\lambda(z_k^\lambda) = z_{k-1}^\lambda$ and so $F_\lambda^{k-1}(z_k^\lambda) = 0$. Now the points z_k^λ vary analytically with λ and are strictly contained in the interior of R^λ. So we may consider the function $H^k(\lambda)$ defined on $\mathcal{O}'$ by $H^k(\lambda) = v_0^\lambda - z_k^\lambda$ where $v_0^\lambda = F_\lambda(c_0^\lambda)$. When λ rotates once around the boundary of $\mathcal{O}'$, v_0^λ rotates once around the boundary of R^λ while z_k^λ remains in the interior of R^λ. Hence $H^k(\lambda)$ has winding number one along the boundary of $\mathcal{O}'$ and so there must be a unique zero in $\mathcal{O}'$ for each H^k. This is then the parameter that lies at the center of the escape time region $\mathcal{E}^k$. It is well known [13] that $\mathcal{E}^k$ is an open disk in the parameter plane. Note that, as λ decreases along $\mathbb{R}^-$, both v_0^λ and z_k^λ increase along $\mathbb{R}^+$. It then follows that the portion of $\mathcal{E}^{k+1}$ in $\mathbb{R}^-$ lies to the left of $\mathcal{E}^k$ in the parameter plane.

To prove the existence of the Mandelbrot sets $\mathcal{M}^k$, recall that the orbit of the point z_k^λ under F_λ remains in R^λ before entering T_λ and landing at 0 at iteration $k-1$ (here $z_2^\lambda = p_2^\lambda$). For each $k \geq 2$, let E_λ^k be the open set surrounding z_k^λ in R^λ that is mapped onto T_λ by F_λ^{k-1}. Let D_λ^k be the set in R^λ consisting of points whose first $k-2$ iterations lie in R^λ but whose $(k-1)^{\text{st}}$ iterate lies in the interior of L^λ. Since F_λ is univalent on R^λ, each D_λ^k is an open disk. Furthermore, the boundary of D_λ^k meets a portion of the boundaries of both E^{k-1} and E^k (where $E_\lambda^1 = T_\lambda$). Since F_λ^{k-1} maps D_λ^k

one-to-one over the interior of L^λ and then F_λ maps L^λ two-to-one over a region that contains R^λ, we have that F_λ^k maps D_λ^k two-to-one over a region that completely contains R^λ. Moreover, the critical value for F_λ^k is just v_0^λ, which, by the preceding Proposition, winds once around the exterior of R^λ as λ winds once around the boundary of $\mathcal{O}'$. Hence F_λ^k is a polynomial-like map of degree two on D_λ^k and this proves the existence of a baby Mandelbrot set $\mathcal{M}^k$ lying in $\mathcal{O}'$ for each $k \geq 2$. When λ is real and negative, we have that the centers of the escape regions $\mathcal{E}^k$ lie along $\mathbb{R}^-$ and, since the real line is invariant under F_λ when $\lambda \in \mathbb{R}^-$, both c_0^λ and v_0^λ also lie on the real axis. Then, by the $\lambda \mapsto \overline{\lambda}$ symmetry in the parameter plane, the spines of these Mandelbrot sets also lie in $\mathbb{R}^-$.

Next, since the E_λ^k and D_λ^k are arranged along the postive real axis in the following fashion:

$$T_\lambda = E_\lambda^1 < D_\lambda^2 < E_\lambda^2 < D_\lambda^3 < E_\lambda^3 < \dots$$

we have that the $\mathcal{E}^k$ and $\mathcal{M}^k$ are arranged along the negative real axis in the parameter plane in the opposite manner:

$$\dots \mathcal{E}^3 < \mathcal{M}^3 < \mathcal{E}^2 < \mathcal{M}^2 < \mathcal{E}^1.$$

See Figure 3.

Finally, when $\lambda \in \mathbb{R}^-$, there is a non-empty interval lying between each adjacent $\mathcal{M}^k$ and $\mathcal{E}^j$ (where $j = k$ or $k-1$). This interval contains parameters for which $F_\lambda^k(c_0^\lambda)$ lies in L^λ, but then $F_\lambda^{k+1}(c_0^\lambda)$ is back in R^λ and close to ∂B_λ. As a consequence, it takes more than k additional iterations for this critical orbit to reach T_λ or return to L^λ.

□

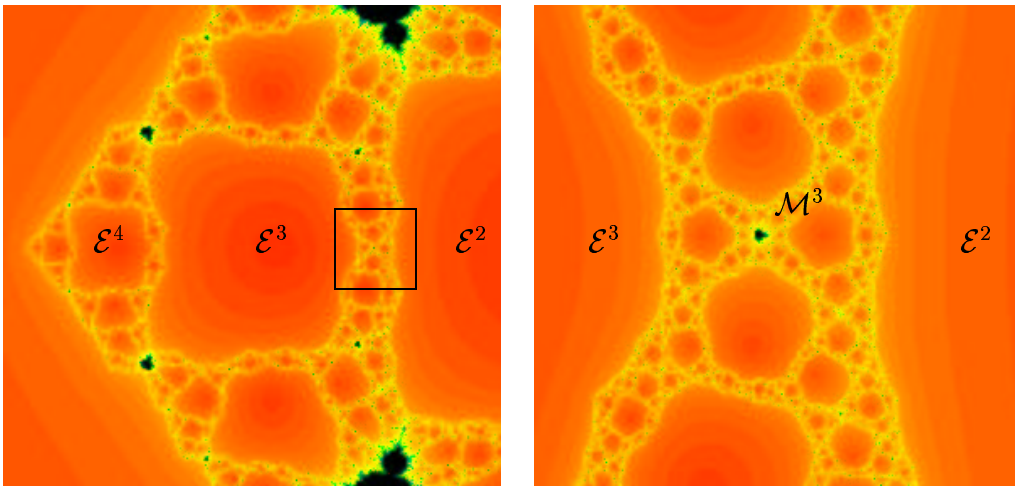

Figure 3: The SM arc along the negative real axis. The $\mathcal{M}^k$ are so small that they are not visible in this picture. However, the magnification shows $\mathcal{M}^3$.

3 Phase Two

In this second phase of the construction of the MS maze, we shall show that, on each side of the Mandelbrot set $\mathcal{M}^k$ in the first SM arc, there are a pair of infinite SM arcs, each extending over to one of the adjacent Sierpinski holes $\mathcal{E}^k$ and $\mathcal{E}^{k-1}$. In addition, there are a pair of finite SM arcs extending above and below each $\mathcal{M}^k$ in the previous SM arc. Here a finite SM arc means that there are only finitely many Mandelbrot sets and Sierpinski holes that alternate along this arc.

To begin this phase of the construction, let us assume that the critical value v_0^λ now lies in a particular open disk D_λ^k for some fixed $k \geq 2$. Let $\mathcal{O}_k \subset \mathcal{O}'$ denote the set of parameters for which this happens. Now the boundary of D_λ^k is mapped by F_λ^{k-1} one-to-one onto the boundary of L^λ, and the boundary of L^λ varies analytically with λ. So we can construct a natural

parametrization of this boundary which also varies analytically with λ. Then we can pull back this parameterization to the boundary of each D_λ^k. Again, as we saw earlier, as λ rotates around the boundary of the original disk $\mathcal{O}'$ in the parameter plane, v_0^λ rotates once around the boundary of R^λ. Hence, arguing just as in the previous section, there must be a unique parameter λ for which v_0^λ lands on any given point in the parametrization of the boundary of D_λ^k. Hence we have that $\mathcal{O}_k$ is a disk contained inside $\mathcal{O}'$ and, as λ rotates once around the boundary of $\mathcal{O}_k$, the critical value has winding number one around the boundary of the disk D_λ^k.

Now consider the set of preimages in L^λ of all of the D_λ^j and E_λ^j under F_λ. Since we have assumed that v_0^λ lies in D_λ^k, it follows that there is a unique preimage of D_λ^k in L^λ which is a disk that contains c_0^λ and is mapped two-to-one onto D_λ^k. For each other D_λ^j (with $j \neq k$), there are two preimage disks lying in L^λ. Note that, when $\lambda \in \mathbb{R}^-$ and $j > k$, there are a pair of preimages of D_λ^j lying along $\mathbb{R}^-$, one to the right of the preimage of D_λ^k and one to the left. These preimages tend away from D_λ^k in either direction as j increases. When $2 \leq j < k$, there are again two preimages of D_λ^j, but when $\lambda \in \mathbb{R}^-$, these preimages no longer lie on the negative axis; rather they branch out more or less perpendicularly above and below the preimage of D_λ^k on this axis. As for the preimages of E_λ^j in L^λ, we have the same situation: there are infinitely many pairs of preimages of each E_λ^j lying along $\mathbb{R}^-$ on either side of the preimage of D_λ^k when $j \geq k$ and $\lambda \in \mathbb{R}^-$, and finitely many pairs extending above and below this preimage when $1 \leq j < k$. Thus we have a pair of infinite chains of of alternating preimages of the disks D_λ^k and E_λ^k extending away from the preimage of D_λ^k containing c_0^λ and another pair of chains consisting of finitely many such preimages extending in a "perpendicular" direction away from the preimage of D_λ^k.

Since F_λ^{k-1} maps D_λ^k one-to-one over L^λ, we thus have a similar collection

of preimages that lie inside the disk D_λ^k. We denote by D_λ^{kj} each of the two disks in D_λ^k that are mapped onto D_λ^j by F_λ^k when $j \neq k$. And we let D_λ^{kk} denote the single preimage of D_λ^k under F_λ^k that is contained in D_λ^k. So points in D_λ^{kj} have orbits that remain in R^λ for the first $k-2$ iterations, then map to L^λ under the next iteration, and then map into D_λ^j under the next iteration. Then F_λ^{j-1} maps this set onto L^λ. So F_λ^{k+j-1} maps D_λ^{kj} one-to-one onto all of L^λ (assuming $k \neq j$). Then the next iteration takes this set two-to-one onto all of R^λ. Thus the critical value for F_λ^{k+j} is again v_0^λ, and, as we showed above, as λ rotates around the boundary of $\mathcal{O}_k$, v_0^λ circles around the boundary of D_λ^k. Hence F_λ^{j+k} is polynomial-like of degree two on each of the two disks D_λ^{kj} (where we again emphasize that we are assuming $j \geq 2$ and $j \neq k$). So this produces a pair of Mandelbrot sets $\mathcal{M}^{kj}$ with base period $k+j$ in $\mathcal{O}_k$. As in the previous construction, the Mandelbrot sets $\mathcal{M}^{kj}$ with $j > k$ all have spines lying along $\mathbb{R}^-$, one on each side of $\mathcal{M}^k$. The other Mandelbrot sets with $j < k$ now lie off the real axis, one above $\mathcal{M}^k$ and the other below $\mathcal{M}^k$.

Similar arguments as in the preceding section also produce a pair of Sierpinski holes $\mathcal{E}^{kj}$ on each side of $\mathcal{M}^k$ whose centers lie on the real axis where now $j \geq k$. And there are a pair of Sierpinski holes $\mathcal{E}^{kj}$, one above and one below $\mathcal{M}^k$, where now $1 \leq j < k$. As earlier, these Mandelbrot sets and Sierpinski holes alternate along each of these SM arcs. For parameters in the Sierpinski hole $\mathcal{E}^{k1}$, the critical orbit $F_\lambda^i(c_0^\lambda)$ lies in R^λ for iterations $1 \leq i \leq k-1$. Then $F_\lambda^k(c_0^\lambda)$ returns to L^λ, and then $F_\lambda^{k+1}(c_0^\lambda)$ enters T_λ.

Note that the Mandelbrot sets $\mathcal{M}^{kj}$ are not subsets of the larger Mandelbrot set $\mathcal{M}^k$. This follows since the orbit of the critical point returns to L^λ only at iterations k and $k+j$ when $\lambda \in \mathcal{M}^{kj}$, whereas these returns occur at iterations k and $2k$ when $\lambda \in \mathcal{M}^k$. This also follows from the fact that there is a Sierpinski hole separating each of these baby Mandelbrot sets from $\mathcal{M}^k$

along the new SM arc. In Figure 4 we display a portion of these smaller SM arcs around $\mathcal{M}^4$. To summarize the results at this phase of the construction, we have shown:

Theorem. *In the original SM arc, between each $\mathcal{E}^{k-1}$ and $\mathcal{E}^k$, there exist a pair of infinite SM arcs, each containing Mandelbrot sets $\mathcal{M}^{kj}$ where $j > k$ and Sierpinski holes $\mathcal{E}^{kj}$ where $j \geq k$ in the same alternating arrangement as earlier. One SM arc extends from $\mathcal{M}^k$ to $\mathcal{E}^{k-1}$, the other from $\mathcal{M}^k$ to $\mathcal{E}^k$. The are also a pair of finite SM arcs extending away from $\mathcal{M}^k$ in opposite directions. These finite arcs contain the Mandelbrot sets $\mathcal{M}^{kj}$ where $2 \leq j < k$ and the Sierpinski holes $\mathcal{E}^{kj}$ where now $1 \leq j < k$. The Mandelbrot sets $\mathcal{M}^{kj}$ have base period $k + j$ and the Sierpinski holes $\mathcal{E}^{kj}$ have escape time $k + j$.*

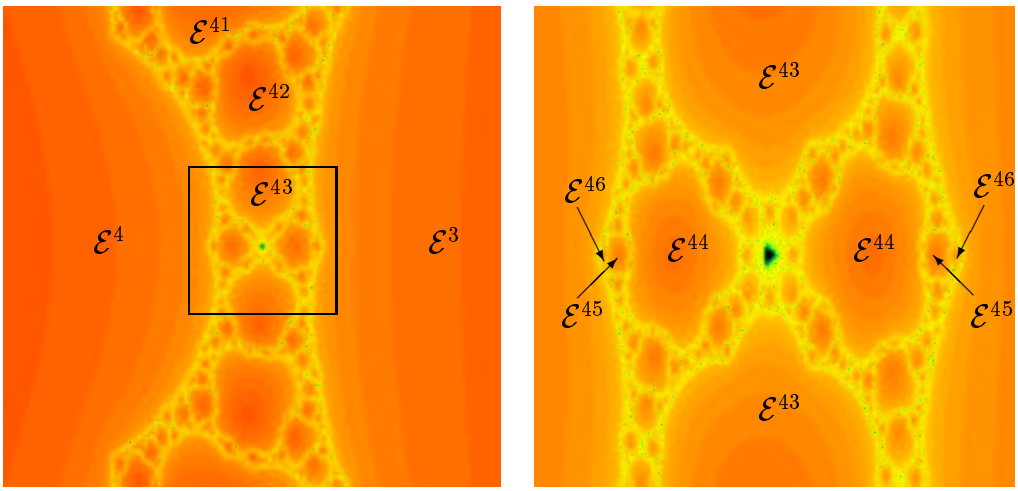

Figure 4: The finite SM arc above and below $\mathcal{M}^4$ as well as a magnification along the real axis.

Geometrically, we think of this second portion of the maze as a "plus sign" since the two infinite SM arcs branch away from $\mathcal{M}^k$ in opposite di-

rections while the finite SM arcs branch away in each of the "perpendicular" directions. Note that this second portion of the maze can also be obtained as follows. We choose a particular Mandelbrot set from the previous portion of the construction. Then this set divides the current portion of the maze into two distinct pieces, one on each side of the given Mandelbrot set. Then, in a small enough neighborhood of this Mandelbrot set, we duplicate each of these pieces and place the duplicated pieces on opposite sides of the given Mandelbrot set, with the rotation between the different pairs given by a quarter of a turn.

4 Final Phase

In this section we complete the construction of MS maze. Basically, the remainder of this construction proceeds by induction. To keep the notation simple, we will just describe the next phase of the inductive process. All subsequent phases follow the same pattern.

In the previous construction, we produced a pair of infinite SM arcs emanating from each given $\mathcal{M}^k$ and another pair of finite SM arcs, each joined as a "plus sign" through $\mathcal{M}^k$. At the next stage, we zoom in on one of the Mandelbrot sets $\mathcal{M}^{kj}$ produced in the second phase and then replicate the construction of the abutting finite and infinite SM arcs, only now there will be twice as many such arcs.

As a remark, we assume here that $j \neq k$. The case where $j = k$ is different and produces what we call Mandelpinski spokes in the parameter plane. See [8].

Recall that, for each $\lambda \in \mathcal{O}_k$, the critical value v_0^λ lies in D_λ^k. Let U_λ^k be the preimage of D_λ^k in L^λ that contains c_0^λ. In the previous construction, for each $j > 1$ and $j \neq k$, we produced a pair of disks $D_\lambda^{kj} \subset D_\lambda^k$, and then we

showed that F_λ^{k+j} was a polynomial-like map of degree two on D_λ^{kj}. This generated a pair of Mandelbrot sets that we called $\mathcal{M}^{jk}$. So fix k and j and concentrate on one of the two disks D_λ^{kj} and hence, in the parameter plane, on the corresponding Mandelbrot set $\mathcal{M}^{kj}$. As in the previous step, we now assume that v_0^λ lies in this disk D_λ^{kj}. This is possible since we have shown that v_0^λ winds once around the boundary of D_λ^k as λ winds around $\partial\mathcal{O}_k$, and $D_\lambda^{kj} \subset D_\lambda^k$. Let $\mathcal{O}_{kj}$ be the set of parameters for which this occurs. Then F_λ^{j+k-1} maps D_λ^{kj} one-to-one over L^λ. Thus we can pull back the earlier parametrization of the boundary of L^λ to construct an analytic parameterization of the boundary of D_λ^{kj}. Just as before, there then exists a unique λ in the boundary of $\mathcal{O}_{kj}$ for which v_0^λ lands on a given point on this parametrized boundary curve. Hence v_0^λ winds once around the boundary of the disk D_λ^{kj} as λ winds once around the boundary of $\mathcal{O}_{kj}$.

Since v_0^λ lies in D_λ^{kj}, there is then a preimage of the structure of all of the disks $D_\lambda^{k\ell}$ and $E_\lambda^{k\ell}$ contained in D_λ^k that now lies in the preimage of D_λ^k in L^λ. Each $D_\lambda^{k\ell}$ and $E_\lambda^{k\ell}$ now has two preimages in L^λ, with the exception of the chosen D_λ^{kj}, which has only one preimage that contains the critical point c_0^λ. Thues we again "duplicate" the preimage structure that we see in D_λ^k in the region L^λ, and center this duplication around the preimage of D_λ^{kj}. Then F_λ^{k+j-1} maps the disk D_λ^{kj} one-to-one onto L^λ since $j \neq k$. Hence there is a copy of this duplicated preimage structure that we see in L^λ that is now contained in the chosen disk D_λ^{kj}. Thus, for each $\ell > 1$, we now have four disks named $D^{kj\ell}$ that are contained in D_λ^{kj}. Each of the $D_\lambda^{kj\ell}$ is mapped one-to-one onto L^λ by $F_\lambda^{k+j+\ell-1}$ and hence two-to-one over themselves by $F_\lambda^{k+j+\ell}$. Then, arguing as before, this map is polynomial-like of degree two on each $D^{kj\ell}$ and this produces four new baby Mandelbrot sets $\mathcal{M}^{jl\ell}$ which are arranged in a similar pattern as the preimages of the disks in the dynamical plane. Similar arguments also yield four Sierpinski holes $\mathcal{E}^{jk\ell}$.

Note also that the maze structure in the small neighborhood of $\mathcal{M}^{kj}$ is now more complicated. For example, if we had chosen the disk D_λ^{kj} to be one of the disks in one of the two finite chains of disks emanating from D_λ^k, then the maze structure around $\mathcal{M}^{kj}$ would consist of a pair of finite SM arcs, one on each side of $\mathcal{M}^{kj}$, and also a pair of "plus signs," each again on opposite sides of $\mathcal{M}^{kj}$. On the other hand, had D_λ^{kj} been chosen to be one of the disks in the infinite string of disks, then there would now be a pair of infinite SM arcs emanating from $\mathcal{M}^{kj}$ and again a pair of "plus signs."

Then we may continue this process, each time selecting a previously constructed Mandelbrot set with itinerary $s_0 \dots s_n$. Assuming the sequence $s_0 \dots s_n$ is not a repeated finite sequence, i.e., not a repeating sequence of the form $s_0 \dots s_j \dots s_0 \dots s_j$, this inductive process then produces the more intricate maze structure around the given Mandelbrot set.

5 The General Case

In this section we extend the construction of the Mandelpinski maze to the more general family

$$F_\lambda(z) = z^n + \frac{\lambda}{z^d}$$

where n is even and d is odd and $n, d \geq 2$. We exclude the case where $n = 2$ and $d = 3$ since that was completely covered earlier.

Recall that the $n + d$ critical points of F_λ are given by

$$c^\lambda = \left(\frac{d\lambda}{n}\right)^{\frac{1}{n+d}}$$

and the corresponding critical values given by

$$v_0^\lambda = \frac{(d+n)\lambda^{\frac{n}{n+d}}}{d^{\frac{d}{n+d}} n^{\frac{n}{n+d}}}.$$

There are also $n+d$ prepoles given by

$$p^\lambda = (-\lambda)^{\frac{1}{n+d}}.$$

As mentioned earlier, there is $(n-1)$-fold symmetry in the parameter plane for these maps. And, as shown in [1], there are $n-1$ principal Mandelbrot sets in the parameter plane whose spines lie along the rays that pass through the $(n-1)^{\text{st}}$ roots of unity. So we shall restrict attention only to parameters that are drawn from one of these symmetry sectors, namely the sector $\mathcal{S}$ in the parameter plane that contains the negative real axis and is bounded above and below by the spines of the adjacent principal Mandelbrot sets. More precisely, this sector is given by

$$\frac{(n/2)-1}{n-1} \leq \frac{\operatorname{Arg}\lambda}{2\pi} \leq \frac{n/2}{n-1}.$$

As in Section 2, we may find constants $\alpha < 1$ and $\beta > 1$ such that, if $\lambda \in \mathcal{S}$ and $|\lambda| = \alpha$, then λ lies in the McMullen domain, whereas if $|\lambda| = \beta$, then λ lies in the Cantor set locus. Furthermore, we may construct a round annulus $\mathcal{A}$ in the dynamical plane that encircles the origin and has the property that, if $|\lambda| = \alpha$, then v_0^λ lies on the inner circular boundary of $\mathcal{A}$, whereas if $|\lambda| = \beta$, then v_0^λ lies on the outer circular boundary of $\mathcal{A}$. And, just as in the Proposition in Section 2, we may arrange that, if $\alpha \leq |\lambda| \leq \beta$, then F_λ maps both the inner and outer boundary of $\mathcal{A}$ strictly outside $\mathcal{A}$. We then define the region $\mathcal{O}$ in the parameter plane to be the set of parameters λ in $\mathcal{S}$ that satisfy $\alpha \leq |\lambda| \leq \beta$. See Figure 5 for a picture of this region in the parameter plane when $n = 4$ and $d = 3$.

We now define the analogous sectors L^λ and R^λ in the dynamical plane when $\lambda \in \mathcal{O}$. First, when $\lambda \in \mathbb{R}^-$, L^λ is the region that is contained in the annulus $\mathcal{A}$ and bounded by the two prepole rays given by

$$\frac{\operatorname{Arg} z}{2\pi} = \frac{1}{2} \pm \frac{1}{2(n+d)}.$$

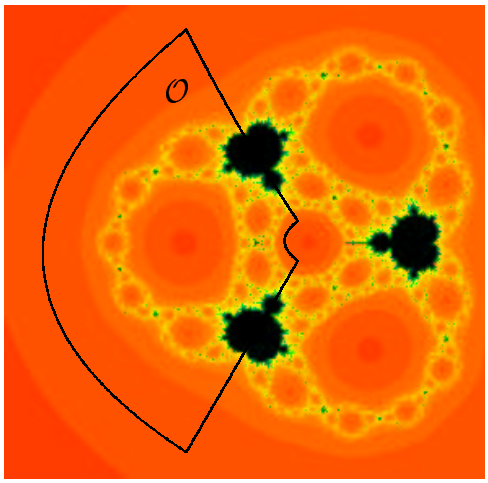

Figure 5: The symmetry sector $\mathcal{O}$ when $n = 4$ and $d = 3$.

The sector R^λ is also contained in $\mathcal{A}$ and is bounded by the two critical point rays given by

$$\frac{\operatorname{Arg} z}{2\pi} = \pm\frac{1}{2(n+d)}.$$

As λ rotates through $\mathcal{O}$ in the clockwise (resp., counterclockwise) direction by $1/(2(n-1))$ of a turn, the critical points and prepoles on the straightline boundaries of these sectors each rotate by exactly $1/(2(n-1)(n+d))$ of a turn in the clockwise (resp., counterclockwise) direction. As a consequence, as λ rotates around $\mathcal{O}$ in the clockwise direction, the upper boundary of R^λ ends up on the line

$$\frac{\operatorname{Arg} z}{2\pi} = \frac{1}{2(n+d)} - \frac{1}{2(n-1)(n+d)}$$

whereas, when λ rotates around $\mathcal{O}$ in the counterclockwise direction, the upper straightline boundary of L^λ moves to the line given by

$$\frac{\operatorname{Arg} z}{2\pi} = \frac{1}{2} + \frac{1}{2(n+d)} + \frac{1}{2(n-1)(n+d)}.$$

As described earlier, there is a single critical point in the interior of L^λ denoted by c_0^λ. The image of c_0^λ is the critical value denoted by v_0^λ. Our goal is to show:

Proposition. *For each $\lambda \in \mathcal{O}$:*

- *F_λ maps R^λ one-to-one over $R^\lambda \cup L^\lambda$ plus a portion of T_λ containing 0;*
- *F_λ maps L^λ two-to-one over R^λ;*
- *As λ winds once around the boundary of $\mathcal{O}$, the critical value v_0^λ winds once around R^λ.*

Then, using the exact same techniques as in Section 2, this proves the existence of the initial part of the maze, which consists of alternating Sierpinski holes and Mandelbrot sets

$$\cdots < \mathcal{E}^3 < \mathcal{M}^3 < \mathcal{E}^2 < \mathcal{M}^2 < \mathcal{E}^1$$

along the negative real axis.

To prove the first part of this result, we need to show that the images of the critical point rays that bound R^λ lie outside both R^λ and L^λ. Let v^λ be the critical value that is the image of the critical point c^λ that lies on the upper straightline boundary of R^λ. We claim that v^λ lies strictly between the sectors L^λ and R^λ, as long as $n > 2$. When $n = 2$, we have that this critical value may lie along one of the straight line boundaries of these sectors, just as we saw in the case $n = 2, d = 3$.

When $\lambda \in \mathbb{R}^-$, we have

$$\frac{\operatorname{Arg} c^\lambda}{2\pi} = \frac{1}{2(n+d)} \quad \text{and} \quad \frac{\operatorname{Arg} v^\lambda}{2\pi} = \frac{n}{2(n+d)}.$$

As λ rotates between the pair of principal Mandelbrot sets in $\mathcal{O}$, the argument of v^λ satisfies

$$\frac{n}{2(n+d)} - \frac{n}{2(n-1)(n+d)} \leq \frac{\operatorname{Arg} v^\lambda}{2\pi} \leq \frac{n}{2(n+d)} + \frac{n}{2(n-1)(n+d)}.$$

Using the above locations of the boundaries of L^λ and R^λ, we must therefore show that the position of v^λ relative to R^λ after a clockwise rotation is

$$\frac{1}{2(n+d)} - \frac{1}{2(n-1)(n+d)} \leq \frac{n}{2(n+d)} - \frac{n}{2(n-1)(n+d)}$$

and also that the position of v^λ relative to L^λ after the counterclockwise rotation is

$$\frac{n}{2(n+d)} + \frac{n}{2(n-1)(n+d)} \leq \frac{1}{2} + \frac{1}{2(n+d)} + \frac{1}{2(n-1)(n+d)}.$$

Straightforward algebra then shows that these inequalities both hold. Moreover, these inequalities are strict when $n > 2$. When $n = 2$, the only place where we get equality is when λ lies along the spines of the principal Mandelbrot sets that bound the region $\mathcal{O}$. Then the arguments given earlier for the case $n = 2$ and $d = 3$ hold for any d when $n = 2$.

A similar argument shows that the critical value that is the image of the critical point that lies on the lower straightline boundary of R^λ now lies in the lower half plane but again between the sectors R^λ and L^λ as λ rotates through $\mathcal{O}$.

Since the outer and inner circular boundaries of R^λ are mapped onto a simple closed curve in B_λ that surrounds $L^\lambda \cup R^\lambda$, we therefore have that F_λ maps R^λ one-to-one over $L^\lambda \cup R^\lambda$. In addition, there is a region in R^λ that is mapped onto a neighborhood of 0 in T_λ.

For the second case, recall that the straightline boundaries of L^λ contain two prepoles, p_+^λ in the upper boundary and p_-^λ in the lower boundary. The prepole rays passing through these two points are then mapped onto straight

lines that pass through the origin and extend to ∞ in both directions. Let ℓ_+^λ (resp., ℓ_-^λ) be the line that is the image of the prepole ray containing p_+^λ (resp., p_-^λ).

When $\lambda \in \mathbb{R}^-$, we have

$$\frac{\operatorname{Arg} p_+^\lambda}{2\pi} = \frac{1}{2} - \frac{1}{2(n+d)} \quad \text{and} \quad \operatorname{Arg} \frac{p_-^\lambda}{2\pi} = \frac{1}{2} + \frac{1}{2(n+d)}.$$

Then we have

$$\frac{\operatorname{Arg} \ell_+^\lambda}{2\pi} = \frac{n}{2} - \frac{n}{2(n+d)} = -\frac{n}{2(n+d)}.$$

We shall consider only the portion of the line ℓ_+^λ that lies in the upper half plane, so we then have

$$\frac{\operatorname{Arg} \ell_+^\lambda}{2\pi} = \frac{1}{2} - \frac{n}{2(n+d)} = \frac{d}{2(n+d)}.$$

We also have

$$\frac{\operatorname{Arg} \ell_-^\lambda}{2\pi} = \frac{n}{2(n+d)}.$$

As λ rotates in the counterclockwise direction to the lower principal Mandelbrot set in $\mathcal{O}$, the line ℓ_+^λ moves to

$$\frac{\operatorname{Arg} \ell_+^\lambda}{2\pi} = \frac{d}{2(n+d)} + \frac{n}{2(n-1)(n+d)}$$

while the line ℓ_-^λ moves to

$$\frac{\operatorname{Arg} \ell_-^\lambda}{2\pi} = \frac{n}{2(n+d)} + \frac{n}{2(n-1)(n+d)}.$$

As λ rotates in the clockwise direction to the upper principal Mandelbrot set in $\mathcal{O}$, the line ℓ_+^λ moves to

$$\frac{\operatorname{Arg} \ell_+^\lambda}{2\pi} = \frac{d}{2(n+d)} - \frac{n}{2(n-1)(n+d)}$$

while the line ℓ_-^λ moves to

$$\frac{\operatorname{Arg} \ell_-^\lambda}{2\pi} = \frac{n}{2(n+d)} - \frac{n}{2(n-1)(n+d)}.$$

So we have to show that portions of the lines $\ell_\pm^\lambda$ in the upper and lower half planes are contained between the boundaries of L^λ and R^λ for all parameters in $\mathcal{O}$. First consider the upper half plane case. Let γ be either n or d. Then, for the case of L^λ, we need to show that

$$\frac{\gamma}{2(n+d)} + \frac{n}{2(n-1)(n+d)} \leq \frac{1}{2} + \frac{1}{2(n+d)} - \frac{1}{2(n-1)(n+d)}.$$

But this is equivalent to

$$\frac{n}{2(n-1)} \leq \frac{\gamma}{2} + \frac{1}{2} - \frac{1}{2(n-1)}$$

or, more simply,

$$\frac{n+1}{n-1} \leq \gamma + 1.$$

Thus, as usual, when $\gamma = n = 2$, we get equality in the above expression. But for all other values of n and d, this is a strict inequality, i.e., the lines $\ell_\pm^\lambda$ lie strictly to the right of the upper boundary of L^λ.

For the case R^λ, we need to show

$$\frac{\gamma}{2(n+d)} - \frac{n}{2(n-1)(n+d)} \geq \frac{1}{2(n+d)} - \frac{1}{2(n-1)(n+d)}.$$

But this is now equivalent to

$$\gamma - \frac{n}{n-1} \geq 1 - \frac{1}{n-1}$$

which yields

$$\gamma - \frac{n-1}{n-1} \geq 1$$

which is true for any n and d. As always, we get strict inequality here for any d and $n > 2$. Then a similar proof goes through in the lower half plane.

Since n is even and d is odd, the portions of the circular boundaries of L^λ that lie in B_λ and T_λ are both mapped into the portion of B_λ that lies outside of $\mathcal{A}$ and to the right of R^λ. As a consequence, we have that, for each $\lambda \in \mathcal{O}$, F_λ maps L^λ two-to-one over R^λ. This proves the second part of the Proposition.

Finally, recall that v_0^λ is the image of the critical point that lies in L^λ. This critical value lies on the positive real axis when $\lambda \in \mathbb{R}^-$. When λ rotates to the spine of the principal Mandelbrot set in the lower portion of $\mathcal{O}$, we have that

$$\frac{\operatorname{Arg} v_0^\lambda}{2\pi} = +\frac{n}{2(n-1)(n+d)}.$$

Meanwhile, the upper straightline boundary of R^λ for these λ-values is given by

$$\frac{\operatorname{Arg} z}{2\pi} = \frac{1}{2(n+d)} + \frac{1}{2(n-1)(n+d)}.$$

So we have that the argument of the straight line containing v_0^λ is equal to the argument of the upper straightline boundary of R^λ. The same thing occurs when λ lies on the lower straightline boundary of $\mathcal{O}$, only now these straight lines lie in the lower half plane. Also, when λ rotates along each of the two circular boundaries of $\mathcal{O}$, v_0^λ rotates around a half circle in B_λ that lies to the right of R^λ. This proves that F_λ is polynomial-like of degree two on the sector L^λ. This completes the proof of the Proposition.

Without going into details, the remainder of the construction of the Mandelpinski maze presented in Sections 2-4 for the case $n = 2, d = 3$ goes over essentially without change to this more general case.

References

[1] Devaney, R. L. Baby Mandelbrot Sets Adorned with Halos in Families of Rational Maps. In *Complex Dynamics; Twenty-Five Years After*

the Appearance of the Mandelbrot Set. Amer. Math. Soc. Contemporary Math. **396** (2006), 37-50.

[2] Devaney, R. L. Structure of the McMullen Domain in the Parameter Space of Rational Maps. *Fund. Math.* **185** (2005), 267-285.

[3] Devaney, R. L. Singular Perturbations of Complex Polynomials. *Bulletin of the AMS* **50** (2013), 391-429.

[4] Devaney, R. L. Cantor Necklaces and Sierpinski Curve Julia Sets. *Qual. Thy. Dyn. Sys.* **5** (2004), 337-359.

[5] Devaney, R. L. and Look, D. M. A Criterion for Sierpinski Curve Julia Sets. *Topology Proceedings* **30** (2006), 163-179.

[6] Devaney, R. L., Look, D. M., and Uminsky, D. The Escape Trichotomy for Singularly Perturbed Rational Maps. *Ind. Univ. Math. J.* **54** (2005), 1621-1634.

[7] Devaney, R. L. and Russell, E. Connectivity of Julia Sets of Singularly Perturbed Rational Maps. In *Chaos, CNN, Memristors and Beyond.* World Scientific Press (2013), 239-245.

[8] Devaney, R. L. Mandelpinski Spokes in a Family of Rational Maps. To appear.

[9] Douady, A. and Hubbard, J. On the Dynamics of Polynomial-like Mappings. *Ann. Sci. ENS Paris* **18** (1985), 287-343.

[10] McMullen, C. Automorphisms of Rational Maps. *Holomorphic Functions and Moduli.* Vol. 1. Math. Sci. Res. Inst. Publ. **10** Springer, New York, 1988.

[11] Milnor, J. *Dynamics in One Complex Variable.* Princeton University Press, 2006.

[12] Moreno Rocha, M. A Combinatorial Invariant for Escape Time Sierpinski Rational Maps. *Fund. Math.* **222** (2013), 99-130.

[13] Roesch, P. On Captures for the Family $f_\lambda(z) = z^2+\lambda/z^2$. In *Dynamics on the Riemann Sphere.* European Mathematical Society (2006), 121-130.